Low-Voltage Origami-Paper-Based Electrophoretic Device for Rapid Protein Separation

ARTICLE *in* ANALYTICAL CHEMISTRY · DECEMBER 2014

Impact Factor: 5.64 · DOI: 10.1021/ac503976c · Source: PubMed

3 AUTHORS, INCLUDING:

Long Luo
University of Texas at Austin
13 PUBLICATIONS **72** CITATIONS
SEE PROFILE

Xiang Li
University of Texas at Austin
9 PUBLICATIONS **103** CITATIONS
SEE PROFILE

analytical chemistry

Article

pubs.acs.org/ac

Low-Voltage Origami-Paper-Based Electrophoretic Device for Rapid Protein Separation

Long Luo,[†] Xiang Li,[†] and Richard M. Crooks*

Department of Chemistry, The University of Texas at Austin, 105 East 24th Street Stop A5300, Austin, Texas 78712-1224, United States

Supporting Information

ABSTRACT: We present an origami paper-based electrophoretic device (*o*PAD-Ep) that achieves rapid (~5 min) separation of fluorescent molecules and proteins. Due to the innovative design, the required driving voltage is just ~10 V, which is more than 10 times lower than that used for conventional electrophoresis. The *o*PAD-Ep uses multiple, thin (180 μm/layer) folded paper layers as the supporting medium for electrophoresis. This approach significantly shortens the distance between the anode and cathode, and this, in turn, accounts for the high electric field (>1 kV/m) that can be achieved even with a low applied voltage. The multilayer design of the *o*PAD-Ep enables convenient sample introduction by use of a slip layer as well as easy product analysis and reclamation after electrophoresis by unfolding the origami paper and cutting out desired layers. We demonstrate the use of *o*PAD-Ep for simple separation of proteins in bovine serum, which illustrates its potential applications for point-of-care diagnostic testing.

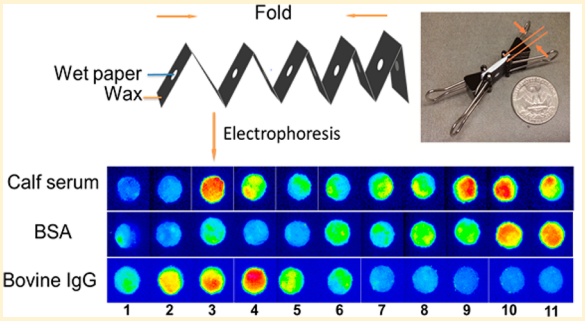

In this article, we introduce a new kind of electrophoretic (Ep) device, which is appropriate for integration into paper analytical devices (PADs),[1,2] and demonstrate separation of fluorescent molecules and proteins at very low voltages. The device, which we call an *o*PAD-Ep (the *o* stands for origami),[3] is very easy to construct (Scheme 1). Briefly, a piece of filter paper is folded into a multilayer structure that serves as the Ep medium. A slip layer is added to introduce the sample,[4] and this assembly is then sandwiched between two Ag/AgCl electrode assemblies. The important new finding is that an electric field of a few kilovolts per meter can be easily generated in an *o*PAD-Ep using an applied voltage of just 10 V due to the thinness of the folded paper (~2 mm thick for an 11-layer origami construct). In contrast, a much higher applied voltage (100–300 V) is required to achieve a similar field using a conventional Ep apparatus.[5] In addition, the multilayer structure of this device offers several important advantages. First, a separate slip layer is easily incorporated in *o*PAD-Ep for sample introduction.[4] The position of the slip layer determines the initial location of sample. Second, product analysis after Ep is easily performed by unfolding the device, and the resolution of product distribution can be as high as the thickness of a single paper layer (~180 μm). Third, after Ep separation, the paper can be cut to reclaim one or multiple components from a complex mixture for further analysis. Finally, the *o*PAD-Ep provides an alternative means for controlled and rapid transport of charged molecules through wetted paper when normal capillary driven flow is absent or too slow. The simple construction, low voltage requirement, and other properties alluded to above may make *o*PAD-Ep suitable for point-of-care (POC) applications, for example, as a component of diagnostic devices.

Scheme 1

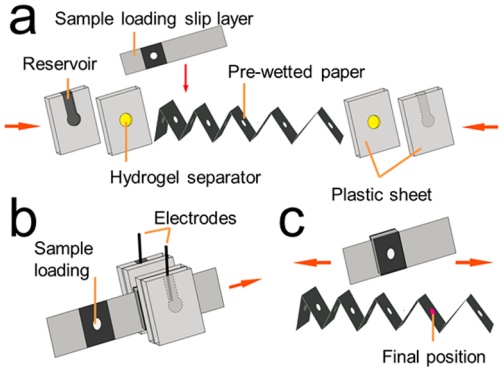

In the 1930s, Tiselius developed the first Ep system, the Tiselius apparatus, for analysis of colloidal mixtures.[6] This technique has evolved over time to take maximum advantage of physical and chemical differences between targets (usually proteins or DNA). For example, the supporting medium may be filter paper,[7] natural gels,[8−12] or synthetic gels,[13] and the apparatuses used to carry out these separations also vary widely

Received: October 24, 2014
Accepted: November 14, 2014
Published: December 2, 2014

(e.g., SDS-PAGE,[14,15] capillary Ep,[16] and isoelectric focusing[17,18]).

In recent years, simple forms of paper Ep have been developed that might eventually find their way into POC devices. For example, Ge et al. introduced a paper-based electrophoretic device for amino acid separation by imitating the design of conventional electrophoretic systems.[19] Using wax printing,[20] they patterned two reservoirs connected by a ∼20 mm long channel on paper. A voltage of 330 V was applied across the channel, which achieved an electromigration speed of a few millimeters per minute for amino acids. Using an alternative design, Chen et al. achieved a similar electric field, but they avoided the necessity of using a high applied voltage by placing the anode and cathode in close proximity (∼2 mm).[21] However, the device designs mentioned above involve either a high voltage, which is not suitable for POC applications, or challenging operational characteristics. Moreover, a constant pH was not maintained in either of these two devices, raising concerns about nonuniform Ep of amphoteric molecules, whose mobilities are strongly dependent on the solution pH. The multilayer *o*PAD-Ep design we describe herein addresses these issues.

Three-dimensional (3D) PADs were first reported by Whitesides and co-workers in 2008.[22] In these devices, multiple paper layers were stacked and held together with double-sided tape. More recently, our group introduced a simpler method for achieving similar functionality by using the fabrication principles of origami, that is, folding a single piece of paper into a 3D geometry.[3] We call this family of sensors *o*PADs. Since their inception, a number of *o*PADs have been reported for various applications, including detection of biomolecules,[23−25] paper-based batteries,[21] and even a microscope.[26] In contrast to earlier systems, the *o*PAD-Ep takes advantage of the thinness of the paper used for device fabrication. This results in a very short distance between the anode and cathode, just a few millimeters, which leads to electric fields of ∼2 kV/m with an input voltage of just 10 V. When subjected to this field, fluorescent molecules or proteins penetrate each paper layer at a speed of 1−3 layers/min. In this article, we discuss the fundamental characteristics of the *o*PAD-Ep design, demonstrate the separation of fluorescent molecules based on their different electrophoretic mobilities, and then show that bovine serum albumin (BSA) can be separated from calf serum within 5 min. We believe that these characteristics are sufficiently desirable that the *o*PAD-Ep will eventually be incorporated into more sophisticated paper diagnostic devices when a separation step is required prior to analysis.

EXPERIMENTAL SECTION

Chemicals and Materials. Tris-HCl buffer (1.0 M, pH 8.0), phosphate buffered saline (PBS, pH 7.4), and Whatman grade 1 chromatography paper were purchased from Fisher Scientific. Silver wire (2.0 mm in diameter), calf serum from formula-fed bovine calves, albumin (lyophilized powder, ≥95%, agarose gel Ep) and IgG (reagent grade, ≥95%, SDS-PAGE, essentially salt-free, lyophilized powder) from bovine serum, and FluoroProfile protein quantification kits were purchased from Sigma-Aldrich. The following fluorescent molecules were used as received: $Ru(bpy)_3Cl_6$ (Fluka), 4,4-difluoro-1,3,5,7,8-pentamethyl-4-bora-3*a*,4*a*-diaza-*s*-indacene ($BODIPY^{2-}$, Invitrogen), 8-methoxypyrene-1,3,6-trisulfonic acid trisodium salt ($MPTS^{3-}$, Anaspec), 1,3,6,8-pyrenetetrasulfonic acid tetrasodium salt (PTS^{4-}, Fisher Scientific), Rhodamine 6G (Acros), methylene blue (Sigma-Aldrich), and rhodamine B (Fluka). All solutions were prepared using deionized water having a resistivity of 18.2 MΩ cm from a Milli-Q Gradient System (Bedford, MA). Serum protein solutions were prepared with PBS.

Device Fabrication. *o*PAD-Eps were fabricated in three steps: (1) the slip layer and origami paper were patterned using wax printing,[20] (2) the plastic buffer reservoirs were fabricated using a laser cutter, and (3) the *o*PAD-Eps were assembled as shown in Scheme 1. Briefly, CorelDraw software was used to design wax patterns on Whatman grade 1 paper (the patterns used for the slip layers and origami sections are provided in the Supporting Information). After wax patterning using a Xerox 8570DN inkjet printer, the paper was placed in an oven at 120 °C for 45 s and then cooled to 25 ± 2 °C. The unwaxed disk in the center of each section of the origami paper was ∼3.5 mm in diameter.

As shown in the Supporting Information, slip layers were partially laminated using Scotch self-sealing laminating pouches from 3M. There are two main reasons for this design. First and foremost, the plastic sheath reduces the friction between slip layer and wetted origami paper so that slipping does not cause serious damage to the paper. Second, it ensures alignment of the sample loading zone on the slip layer with the channel in the origami paper. Similarly, fabrication of buffer reservoirs begins with a design in CorelDraw (Supporting Information). Each reservoir consists of three layers, which are aligned, stacked, and then bound by acrylic adhesive (Weld-On). Each layer was fabricated by cutting a clear 0.32 cm thick acrylic sheet using an Epilog Zing 16 laser cutter (Epilog Laser, Golden, CO). The layer in direct contact with the origami paper has a 6.5 mm diameter hole at its center, and this was filled with a 5.0% agar gel prepared with buffer solution. This gel serves as a separator between the origami paper and reservoir solution, and it prevents the paper from being damaged by long-term exposure to solution, undesirable pH changes, and the effects of pressure-driven flow. After all parts were fabricated, they were assembled into the final device (Scheme 1). Finally, the origami paper was prewetted with buffer solution, and the slip layer was placed in the desired position. The pressure holding the *o*PAD-Ep together is adjustable using four screws at the corners of the plastic sheets: finger-tight torque was found to be optimal.

Operation of the *o*PAD-Ep. Before use, the two reservoirs of the *o*PAD-Ep were filled with 300.0 μL of buffer, and then a Ag/AgCl electrode was inserted into each of them. For fluorescent molecule Ep, 0.20 M Tris-HCl (pH 8.0) was used, whereas PBS (pH 7.4) was used for protein Ep. Ag/AgCl electrodes were prepared by immersing Ag wires in commercial bleach overnight[27] and rinsed thoroughly with DI water before use. The surface of the Ag wires turned dark brown after being oxidized to AgCl. A 0.50 μL aliquot of sample solution was loaded at the designated zone on the slip layer and then introduced by pulling the slip layer into alignment with the origami paper. A BK Precision dc regulated power supply (model 1621A) was used to apply a voltage between the two Ag/AgCl electrodes. After Ep, the buffer and electrodes were removed from the reservoirs, and the screws were loosened to unfold the origami paper for analysis.

Fluorescence Analysis. A Nikon AZ100 multipurpose zoom fluorescence microscope was used to acquire fluorescent images of each *o*PAD-Ep layer, including the slip layer, and ImageJ software (NIH, Bethesda, MD) was used to analyze the

dx.doi.org/10.1021/ac503976c | *Anal. Chem.* 2014, 86, 12390−12397

fluorescence intensity. For protein analyses, we used the FluoroProfile protein quantification kit from Sigma-Aldrich to label proteins with a fluorescent tag.[3] Following Ep, 0.50 μL of FluoroProfile fluorescent reagent solution was spotted onto the origami paper and slip layer, both of which were placed in a humidity chamber for 30.0 min and then taken out and dried for an additional 30.0 min in a dark room. During this time period, epicocconone in the stain solution fully reacts with primary amine groups on proteins, producing a fluorescent conjugate having two excitation maxima at ∼400 and ∼500 nm with emission at 610 nm.[28] An Omega XF204 filter (excitation, 540 nm; emission, 570−600 nm) was used to acquire the fluorescence images of stained proteins in the *o*PAD-Ep.

RESULTS AND DISCUSSION

Electrophoresis of Individual Fluorescent Molecules. In this section, we examine the Ep of single fluorescent molecules, and in the following sections, we will show that *o*PAD-Eps are applicable to more complex tasks including separation of fluorescent molecules and proteins. The fluorescent molecules used for demonstration purposes are listed in Table 1, along with their excitation and emission wavelengths (fluorescence spectra are provided in the Supporting Information) and the corresponding microscope filter sets used for analysis.

Table 1. Spectral Information about the Fluorescence Probes

fluorescent molecules	absorption maximum extinction (nm)	fluorescence maximum emission (nm)	excitation filter (nm)	emission filter (nm)
$Ru(bpy)_3^{2+}$	455	622	420−490	510−700
$BODIPY^{2-}$	492	518	460−500	510−560
$MPTS^{3-}$	401	444	340−380	430−480
PTS^{4-}	374	384	340−380	430−480

A detailed summary of the operation of the *o*PAD-Ep is provided in the Experimental Section. Briefly, however, the paper part of the device is folded, as shown in Scheme 1a, and then compressed by plastic sheets. The two reservoirs are filled with buffer, and a Ag/AgCl electrode is inserted into each of them. Next, an aliquot of sample solution is loaded at the designated zone on the slip layer, and then it is introduced into the *o*PAD-Ep by pulling the slip layer into alignment with the origami paper. Finally, a voltage is applied to the electrodes until the separation is complete, as which time the origami paper is removed, unfolded, and analyzed.

In the first series of experiments, a 23-layer paper device was used to study the migration of $BODIPY^{2-}$. This experiment was carried out by placing a 0.50 μL aliquot of 1.0 mM $BODIPY^{2-}$ onto the slip layer, which was, in turn, placed between the second and third layers of the *o*PAD-Ep, namely, position 3 in Figure 1. Upon application of 10.0 V, Figure 1 shows that $BODIPY^{2-}$ migrates from its initial location toward the cathode by penetrating each layer of the origami paper at a rate of ∼2−3 layers per min. The results show that the distribution of $BODIPY^{2-}$ broadens as a function of separation time: the width of the band increases from ∼2 layers at 0 min to ∼5 layers at 6.0 min. In the absence of the electric field (bottom of Figure 1a), the initial $BODIPY^{2-}$ spot broadens by ∼1 layer after 6.0 min. To demonstrate the importance of the origami construct, and particularly its modest thickness (∼4 mm), we also carried out an Ep experiment in a 2.0 cm long regular paper channel using the same applied voltage (details provided in the Supporting Information). In this case, no Ep transport was observed due to the weak electric field.

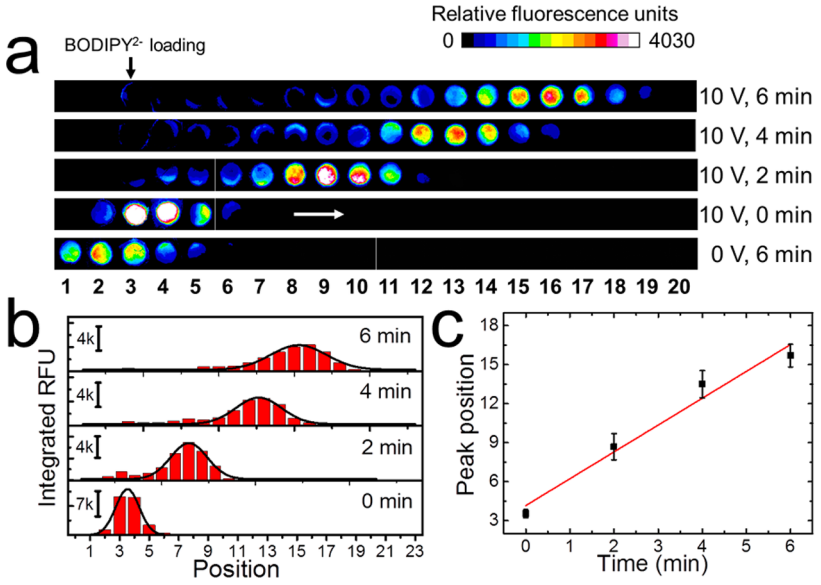

Figure 1. (a) Fluorescence micrographs of a 23-layer *o*PAD-Ep after Ep of $BODIPY^{2-}$ for run times ranging from 0 to 6.0 min at 10.0 V and, in the bottom frame, after 6.0 min with no applied voltage. Fluorescence from just the first 20 layers is shown because the last three layers are at the background level. A 16-level color scale was used to differentiate the fluorescence intensities. $BODIPY^{2-}$ (0.50 μL, 1.0 mM) was initially spotted on the slip layer, which is located at position 3. The white arrow in the fourth micrograph indicates the direction of $BODIPY^{2-}$ migration. (b) Integrated relative fluorescence unit (RFU) distributions, extracted from panel a, as a function of Ep run time. The black line is a Gaussian fit to the histograms. (c) Peak positions derived from the Gaussian fittings in panel b as a function of time. The error bars represent the standard deviation of at least three independent tests at each time.

dx.doi.org/10.1021/ac503976c | *Anal. Chem.* 2014, 86, 12390−12397

To provide a more quantitative analysis of this experiment, the fluorescence intensity (in terms of relative fluorescence units, RFU) of each layer of the *o*PAD-Ep was determined using ImageJ software and then plotted as a function of position in Figure 1b. The standard deviations (σ) and peak positions (μ_0) of the distribution were obtained by fitting the results to a Gaussian distribution. Assuming that diffusion is the major cause of peak broadening, the diffusivity of $BODIPY^{2-}$ in wet paper (D_{paper}) can be roughly estimated using the 1D Einstein diffusion equation (eq 1).

$$\Delta\sigma^2 = 2D_{paper}t \quad (1)$$

Here, $\Delta\sigma^2$ is the mean-square displacement at time t. A plot of σ^2 vs t is provided in the Supporting Information, and from its slope, D_{paper} is calculated to be $\sim 0.14 \times 10^{-9}$ m^2/s, which is about one-third of the diffusivity of $BODIPY^{2-}$ in water ($D_{water} = \sim 0.43 \times 10^{-9}$ m^2/s).[29] This difference may be due to the presence of the network of cellulose fibers that hinders diffusion.[30] This suggests that the peak broadening exhibited by fluorescent molecules in the *o*PAD-Ep is mainly caused by stochastic motion. Two additional points should be mentioned. First, the initial peak broadening observed at 0 min is caused by the sample transfer from the slip layer to the two neighboring layers. Second, there is little or no capillary flow in the *o*PAD-Ep because all layers of the paper are prewetted with the running buffer prior to application of the applied voltage.

Figure 1c shows that there is a linear correlation between the peak position (μ_0) and the time of Ep. The slope of this plot is 2.1 *o*PAD-Ep layers/min, which is equivalent to 6.0 μm/s. Using this value, it is possible to use eq 2 to estimate the Ep mobility (μ_{Ep}) of $BODIPY^{2-}$ in wetted paper (E is the local electric field inside the device). To do so, however, it is necessary to make the simplifying assumption that Ep dominates electroosmosis under the conditions used in our experiments.

$$\mu_{Ep} = \frac{\Delta\mu_0}{E\Delta t} \quad (2)$$

It has been shown previously that the electroosmotic velocity of albumin in barbital buffer in a range of common papers ranges from ~30 to 170% of its Ep velocity at pH 8.8.[31] In addition, Posner and co-workers observed significant electroosmotic flow (EOF) in nitrocellulose paper during their paper-based isotachophoretic preconcentration experiments. Specifically, they found that the fluorescent molecule AF488, which is focused between the leading and trailing electrolytes, moved faster (velocity increased from ~30 to 150 μm/s) after adding 3% poly(vinylpyrrolidone) (PVP) to the leading electrolyte to suppress the EOF.[32] Clearly, the EOF in paper varies over a wide range and is strongly dependent on experimental conditions such as paper structure and electrolyte. Therefore, we measured the electroosmotic velocity of Rhodamine B, which is neutral in the pH range between 6.0 and 10.8,[33] to evaluate the EOF in *o*PAD-Eps under our conditions (details provided in the Supporting Information). The results show that the electroosmotic velocity is small (<0.1 layer/min) compared to Ep and therefore we ignore its contribution in the treatment that follows.

The following procedure was used to determine the value of E. A multimeter was connected in series with the power supply to measure the current flowing through the *o*PAD-Ep with and without origami paper present in the device. At an applied voltage of 10.0 V, the values of the two currents were ~1.7 and 6.0 mA, respectively. Using the difference between these currents and Ohm's law, the calculated resistance of the origami paper is ~4.2 kΩ. By multiplying this resistance by the current at 10.0 V, the voltage drop (ΔV) across the paper is determined to be ~7 V. The value of E in the *o*PAD-Ep (~1.7 kV/m at an applied voltage of 10.0 V) is then calculated by dividing ΔV by the total thickness (d = 4.1 mm) of the 23-layer origami paper. Finally, using eq 2, μ_{Ep} for $BODIPY^{2-}$ in the *o*PAD-Ep is calculated to be $\sim 2.2 \times 10^{-9}$ $m^2/(s\ V)$.

Following the procedure described for $BODIPY^{2-}$, we evaluated the Ep properties of three other dyes in the *o*PAD-Ep: PTS^{4-}, $MPTS^{3-}$, and $Ru(bpy)_3^{2+}$. Plots of the position of these dyes as a function of time are shown in Figure 2. From

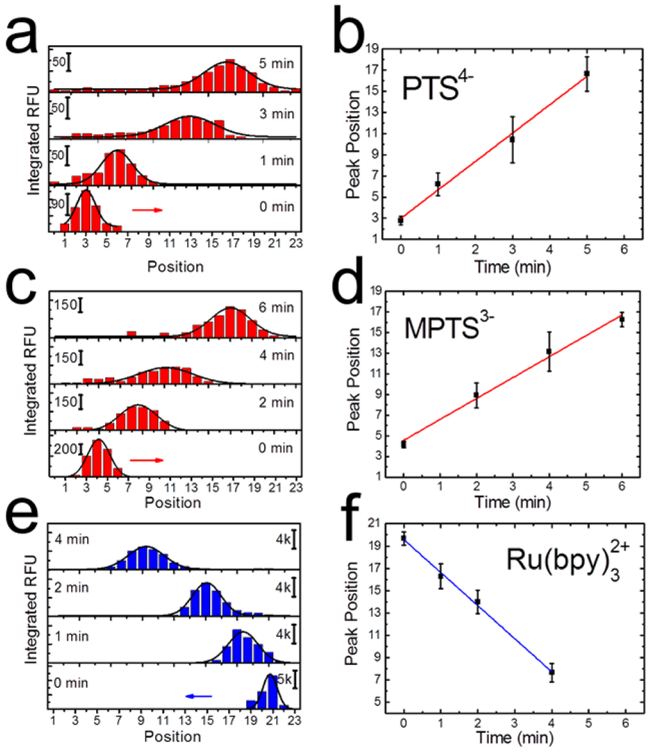

Figure 2. Ep of PTS^{4-}, $MPTS^{3-}$, and $Ru(bpy)_3^{2+}$ using 23-layer *o*PAD-Eps and an applied voltage of 10.0 V for different Ep run times ranging from 0 to 6.0 min. PTS^{4-} or $MPTS^{3-}$ (0.50 μL, 5.0 mM) were initially pipetted onto the slip layer, which is located at position 3. Due to the positive charge of $Ru(bpy)_3^{2+}$, its slip layer is at position 21. (a, c, e) Integrated RFU distributions of these molecules in *o*PAD-Eps as a function of Ep run time. The black lines are Gaussian fits of the histograms. (b, d, f) Peak positions derived from the Gaussian fits in panels a, c, and e as a function of time.

these data, the Ep velocities were determined to be PTS^{4-}, 2.7 layers/min; $MPTS^{3-}$, 2.0 layers/min; and $Ru(bpy)_3^{2+}$, 3.0 layers/min. The corresponding values of μ_{Ep} are 2.9×10^{-9}, 2.1×10^{-9}, and 3.2×10^{-9} $m^2/(s\ V)$, respectively. These mobilities are about 1 order of magnitude smaller than those their counterparts in bulk solution.[34,35] There are several possible reasons for this: hindered migration by the cellulose matrix, specific interactions between the charged molecules and the paper, and small contributions arising from electroosmosis (the direction of EOF is opposite to the migrational direction of negatively charged dyes). Regardless of the underlying phenomena, the relative velocities are $Ru(bpy)_3^{2+}$ > PTS^{4-} >

dx.doi.org/10.1021/ac503976c | *Anal. Chem.* 2014, 86, 12390−12397

$MPTS^{3-}$ ~ $BODPIY^{2-}$. Two other positively charged dyes, Rhodamine 6G (+1 charge between pH 4.0 and 10.0; see Supporting Information)[36] and methylene blue, were also tested and both were found to migrate slowly (<0.2 layer/min) under the same conditions used for the other dyes. This may be a consequence of a strong electrostatic interaction between the negatively charged paper and the positively charged dyes, but why $Ru(bpy)_3^{2+}$ is an exception is still a mystery.

Simultaneous Separation of Multiple Fluorescent Molecules. In this section, two examples are presented that demonstrate separation of fluorescent molecules using the *o*PAD-Ep. The simultaneous first utilizes a mixture of two oppositely charged molecules, $MPTS^{3-}$ and $Ru(bpy)_3^{2+}$, which migrate in opposite directions upon the application of an electric field. The second example demonstrates separation of $BODIPY^{2-}$ and PTS^{4-}, which have the same charge but μ_{Ep} values that differ by about 25%.

The separation of $MPTS^{3-}$ and $Ru(bpy)_3^{2+}$ was carried out as follows. A mixture containing 1.5 mM $MPTS^{3-}$ and 1.5 mM $Ru(bpy)_3^{2+}$ was prepared by mixing equal aliquots of 3.0 mM $MPTS^{3-}$ and 3.0 mM $Ru(bpy)_3^{2+}$, spotting 0.50 μL of the mixture onto the slip layer, and inserting the slip layer at position 11 of the *o*PAD-Ep. All other conditions were the same as those in the previously described single-analyte experiments. When 10.0 V was applied between the two Ag/AgCl driving electrodes, $MPTS^{3-}$ moved from its initial position toward the anode, and $Ru(bpy)_3^{2+}$ migrated toward the cathode. After carrying out the separation, each layer of the *o*PAD-Ep was characterized spectroscopically using a different fluorescence filter (Table 1). Because the emission intensity is different for the two dyes, the results of this experiment, shown in Figure 3a, are normalized by setting the maximum RFU to 1. The key finding is that a near-quantitative separation is achieved in <1 min. Figure 3b shows fluorescence images for the individual dyes (in the same *o*PAD-Ep) 3 min after the application of the voltage. Using the peak positions in Figure 3b, the electrophoretic velocities are ~2 and ~3 layers/min for $MPTS^{3-}$ and $Ru(bpy)_3^{2+}$, respectively. These values are the same as those measured for the individual dyes.

The second demonstration of the *o*PAD-Ep involves the separation of two negatively charged dyes. In this case, a 0.50 μL aliquot of a mixture containing 1.5 mM PTS^{4-} and 0.50 mM $BODIPY^{2-}$ was initially situated at position 3 (Figure 3c,d). Upon application of 10.0 V, both molecules are driven toward the anode and gradually separate (Figure 3c). The calculated Ep velocities of $BODIPY^{2-}$ and PTS^{4-} (Figures 1 and 2, respectively) are 2.1 and 2.7 layers/min. From these values, the predicted peak separation should be ~3–4 paper layers after 5.0 min, which is in good agreement with the value of ~5 layers found in the experiment (Figure 3c,d). Figure 3d shows fluorescence micrographs of $BODIPY^{2-}$ and PTS^{4-} obtained in the same *o*PAD-Ep. The relatively low fluorescence intensity for PTS^{4-} in these experiments is caused by the small Stokes shift of this molecule that does not match perfectly with the fluorescence filter set used (Table 1 and the Supporting Information).

Electrophoresis of Serum Proteins. Ep is widely used to separate biomolecules such as DNA and proteins. One of the most common electrophoretic techniques is gel Ep, which uses a gel to suppress the thermal convection caused by Joule heating and to sieve biomolecules on the basis of their size. This method is routinely used in clinical laboratories to test for abnormalities in a variety of biological matrices, including

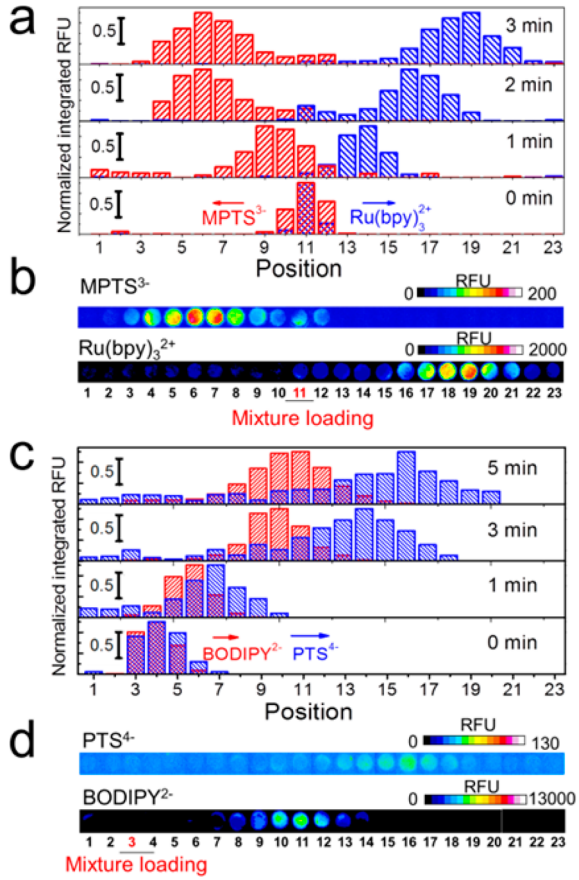

Figure 3. (a) Separation of a mixture of 1.5 mM $MPTS^{3-}$ and 1.5 mM $Ru(bpy)_3^{2+}$ using a 23-layer *o*PAD-Ep and an applied voltage of 10.0 V. A 0.50 μL aliquot of this mixture was initially spotted on the slip layer located at position 11. The two arrows in the fourth histogram indicate the directions of $MPTS^{3-}$ and $Ru(bpy)_3^{2+}$ migration. The blue and red histograms correspond to the distributions of $Ru(bpy)_3^{2+}$ and $MPTS^{3-}$, respectively. (b) Fluorescence micrographs of $MPTS^{3-}$ and $Ru(bpy)_3^{2+}$ in the same *o*PAD-Ep as in panel a after a 3.0 min separation using an applied voltage of 10.0 V. (c) Similar experiment as that in panel a but for a mixture of 1.5 mM PTS^{4-} and 0.50 mM $BODIPY^{2-}$. A 0.50 μL aliquot of this mixture was initially added to the slip layer at position 3. (d) Fluorescence micrographs of PTS^{4-} and $BODIPY^{2-}$ in the same *o*PAD-Ep as that in panel c after 5.0 min Ep at an applied voltage of 10.0 V. Filter sets used to acquire the data are given in Table 1.

serum, urine, blood, and cerebrospinal fluid.[37] For example, in serum protein gel Ep, normal serum is separated into five different bands: (1) albumin, which is approximately two-thirds of the total protein content (3–5 g/dL); (2) alpha-1 (0.1–0.3 g/dL) and (3) alpha-2 (0.6–1.0 g/dL), which are two groups of globulins mainly including heptoglobin, ceruloplasmin, and macroglobin; (4) beta (0.7–1.2 g/dL), composed of transferrin and lipoprotein; and (5) gamma (0.6–1.6 g/dL), which contains primarily immunogolublins such as IgG.[38] An excess or insufficiency in any of these bands may indicate a need for medical attention. Commercially available devices for separating serum proteins usually require a high voltage (200–300 V) and a long separation time (~1 h), both of which are impractical for POC applications. In this section, we will show that the *o*PAD-Ep is able to rapidly (5 min) separate serum proteins using a voltage of just 10 V.

The Ep properties of bovine serum albumin (BSA) and IgG (also from bovine serum) were initially evaluated separately in

dx.doi.org/10.1021/ac503976c | *Anal. Chem.* 2014, 86, 12390–12397

the *o*PAD-Ep. In these experiments, an 11-layer *o*PAD-Ep was first wetted with 1× PBS buffer (ionic strength 163 mM, pH 7.4). Next, 0.50 μL of a 0.1× PBS buffer (ionic strength 16.3 mM) containing either 5.0 g/dL BSA or 1.0 g/dL IgG was loaded at position 3 of the *o*PAD-Ep. These conditions are different from those used for separating the fluorescent molecules: the oPAD-Ep consists of fewer layers (this experimental design flexibility is a noteworthy characteristic of the *o*PAD-Ep) and the buffer concentration is lower, both of which serve to increase the electric field within the device.

Figures 4a shows fluorescence micrographs of BSA in the *o*PAD-Ep before and after the application of 10.0 V for 5.0 min and after 5.0 min in the absence of an electric field. When no voltage is applied, BSA undergoes random diffusion, spreading out by ∼1 layer from the initial position within 5.0 min. In contrast, when 10.0 V is applied, BSA migrates toward the cathode at a speed of ∼1 layer/min (equal to a mobility of ∼5 × 10^{-10} $m^2/(s\ V)$; details are provided in the Supporting Information). The mobility of BSA measured in the *o*PAP-Ep is an order of magnitude lower than the value reported in the literature using conventional paper Ep.[31] In the previously reported experiments, however, Ep was carried out for 14 h (150 times longer than that in our experiments) to achieve a reasonable separation of serum proteins. This long immersion time causes deterioration of the paper structure, which may lead to faster migration of BSA. This contention is supported by the small difference (<8%) between the measured mobility of BSA in paper and in free solution noted in this prior report.[31] In addition, the type of paper and the pH used in our study are different, and the effects of electroosmosis were not considered in our calculation. After migration, remnants of BSA were observed on the paper (positions 6–9, Figure 4a,b), which is expected, as BSA is known as a nonspecific adsorption blocker in paper-based devices.[24]

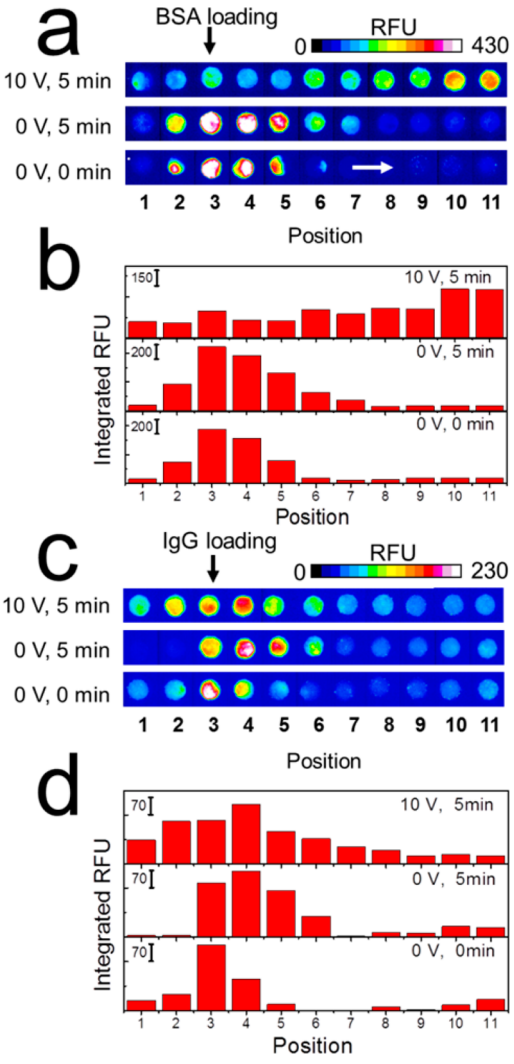

Figure 4. Ep of bovine serum albumin (BSA) and bovine IgG at 10.0 V using 11-layer *o*PAD-Eps. Both BSA and IgG were stained with epicocconone to produce fluorescent conjugates (details provided in the Experimental Section). (a) Fluorescence micrographs of the *o*PAD-Ep after Ep of BSA for 5.0 min at 10.0 V and, in the second and third frames, after 5.0 min and at 0 min with no applied voltage. BSA (0.50 μL, 5.0 g/dL prepared in 0.1× PBS (ionic strength 16.3 mM, pH 7.4)) was initially loaded on the slip layer, which is at position 3. The same procedure was used for a 1.0 g/dL bovine IgG solution, and the fluorescence micrographs are shown in (c). (b, d) Corresponding histograms of integrated RFU extracted from panels a and c, respectively.

In contrast to BSA, the distribution of IgG shifted only slightly toward the anode after 5.0 min, as shown in Figure 4c,d. This is primarily because IgG has a different isoelectric point than BSA: 7.3 ± 1.0[39] and 4.9 ± 0.1,[40,41] respectively (recall that the separation is carried out at pH 7.4). Additionally, IgG is a larger molecule (∼150 kDa) than BSA (∼66.5 kDa),[42] which also leads to a lower mobility.

Applying the same conditions used for the control experiments illustrated in Figure 4, we carried out a separation of the components of calf bovine serum. Figure 5a is a fluorescence micrograph of an *o*PAD-Ep after separation of a 0.50 μL bovine serum sample for 5.0 min at 10.0 V. Two fluorescence maxima are apparent: one near the starting location of the separation (position 3), which belongs to immunoglobulin proteins (including IgG), and the other near positions 9 and 10, corresponding to BSA. By simple visual comparison with the fluorescence intensities of the control experiments shown in Figure 4, it is possible to obtain a quick semiquantitative analysis. The total amount of BSA in the calf serum (Figure 5a) is close to that of the BSA control of 5.0 g/dL (Figure 5b), which lies in the normal range of 3–5 g/dL.[38] Comparison of Figure 5, panels a and c, reveals that the immunoglobulin protein concentration is higher than 1.0 g/dL

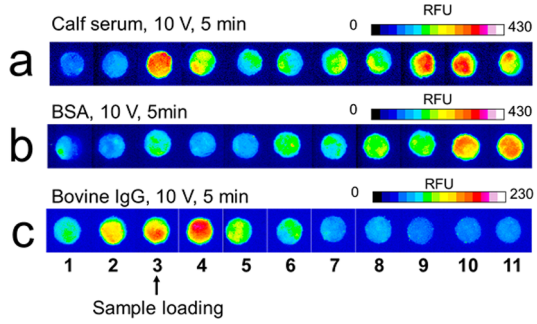

Figure 5. Separation of calf serum in 11-layer *o*PAD-Eps at an applied voltage of 10.0 V. (a) Fluorescence micrographs obtained after Ep of calf serum at 10.0 V for 5.0 min. A 0.50 μL aliquot of serum was initially spotted onto the slip layer at position 3. (b, c) Fluorescence micrographs of *o*PAD-Eps used for single-component control experiments: 5.0 g/dL BSA and 1.0 g/dL bovine IgG, respectively. Separation conditions were the same for all of the data in this figure.

dx.doi.org/10.1021/ac503976c | *Anal. Chem.* 2014, 86, 12390–12397

IgG, but it is still in a reasonable range considering that immunoglobulin proteins other than IgG are also present in the serum sample. A more quantitative analysis is not possible because the fluorescence intensity of protein starts to deviate from linearity at concentrations > ∼0.50 g/dL (a calibration curve is given in the Supporting Information). Also, the other three weak bands, alpha-1, alpha-2, and beta, which usually appear between the immunoglobulin proteins and albumin in conventional serum Ep, cannot be distinguished by the *o*PAD-Ep. This may be because of the strong background of nonspecifically absorbed BSA.

SUMMARY AND CONCLUSIONS

In this article, we have described an innovative design for a low-cost separation system based on folded paper. This approach takes advantage of the thinness of origami paper (180 μm/layer) to achieve a high electric field strength (several kV/m) at a low applied voltage (∼10 V). The voltage required for the *o*PAD-Ep is more than an order of magnitude lower than that used in conventional electrophoretic devices. The simple construction, low voltage requirement, and ease of use make the oPAD-Ep a good candidate for POC applications. Moreover, because it is able to separate fluorescent molecules and serum proteins within ∼5 min, it can potentially be integrated into other types of paper-based devices for preseparation of, for example, blood components.

Currently, we are working on mass spectroscopic analysis of the protein composition on each layer of the device to gain a better understanding of the separation process. Additionally, it may be possible to improve resolution by modifying the paper to reduce nonspecific adsorption. Regardless of these two factors, however, we have shown that the *o*PAD-Ep is effective for certain types of simple separations in low-resource settings.

ASSOCIATED CONTENT

Supporting Information

Design of the *o*PAD-Ep, fluorescence spectra of all fluorescent molecules, paper Ep control experiments, diffusional motion during Ep, Ep of Rhodamine B and Rhodamine 6G, BSA calibration curve, and estimation of BSA mobility. This material is available free of charge via the Internet at http://pubs.acs.org.

AUTHOR INFORMATION

Corresponding Author

*E-mail: crooks@cm.utexas.edu; Tel.: 512-475-8674.

Author Contributions

†L.L. and X.L. contributed equally to this work.

Notes

The authors declare no competing financial interest.

ACKNOWLEDGMENTS

We gratefully acknowledge the National Science Foundation (grant no. 1402242) for support of this project. We also thank the Robert A. Welch Foundation (grant F-0032) for sustained support of our research program.

REFERENCES

(1) Maxwell, E. J.; Mazzeo, A. D.; Whitesides, G. M. *MRS Bull.* **2013**, *38*, 309−314.
(2) Martinez, A. W.; Phillips, S. T.; Whitesides, G. M.; Carrilho, E. *Anal. Chem.* **2010**, *82*, 3−10.
(3) Liu, H.; Crooks, R. M. *J. Am. Chem. Soc.* **2011**, *133*, 17564−17566.
(4) Liu, H.; Li, X.; Crooks, R. M. *Anal. Chem.* **2013**, *85*, 4263−4267.
(5) *Gel Electrophoresis—Principles and Basics*; Magdeldin, S., Ed.; InTech: Rijeka, Croatia, 2012.
(6) Tiselius, A. *Trans. Faraday Soc.* **1937**, *33*, 0524−0530.
(7) Martin, N. H.; Franglen, G. T. *J. Clin. Pathol.* **1954**, *7*, 87−105.
(8) Scopes, R. K. *Biochem. J.* **1968**, *107*, 139−150.
(9) Thorne, H. V. *Virology* **1966**, *29*, 234−239.
(10) Meyers, J. A.; Sanchez, D.; Elwell, L. P.; Falkow, S. *J. Bacteriol.* **1976**, *127*, 1529−1537.
(11) Giri, K. V. *Nature* **1957**, *179*, 632−632.
(12) Bachvaroff, R.; McMaster, P. R. *Science* **1964**, *143*, 1177−1179.
(13) Chrambach, A.; Rodbard, D. *Science* **1971**, *172*, 440−451.
(14) Weber, K.; Osborn, M. *J. Biol. Chem.* **1969**, *244*, 4406−4412.
(15) Schägger, H.; Von Jagow, G. *Anal. Biochem.* **1987**, *166*, 368−379.
(16) Pedersen-Bjergaard, S.; Rasmussen, K. E. *Anal. Chem.* **1999**, *71*, 2650−2656.
(17) Neuhoff, V.; Arold, N.; Taube, D.; Ehrhardt, W. *Electrophoresis* **1988**, *9*, 255−262.
(18) Bjellqvist, B.; Ek, K.; Giorgio Righetti, P.; Gianazza, E.; Görg, A.; Westermeier, R.; Postel, W. *J. Biochem. Biophys. Methods* **1982**, *6*, 317−339.
(19) Ge, L.; Wang, S. W.; Ge, S. G.; Yu, J. H.; Yan, M.; Li, N. Q.; Huang, J. D. *Chem. Commun.* **2014**, *50*, 5699−5702.
(20) Carrilho, E.; Martinez, A. W.; Whitesides, G. M. *Anal. Chem.* **2009**, *81*, 7091−7095.
(21) Chen, S. S.; Hu, C. W.; Yu, I. F.; Liao, Y. C.; Yang, J. T. *Lab Chip* **2014**, *14*, 2124−2130.
(22) Martinez, A. W.; Phillips, S. T.; Whitesides, G. M. *Proc. Natl. Acad. Sci. U.S.A.* **2008**, *105*, 19606−19611.
(23) Liu, H.; Xiang, Y.; Lu, Y.; Crooks, R. M. *Angew. Chem., Int. Ed.* **2012**, *51*, 6925−6928.
(24) Scida, K.; Li, B. L.; Ellington, A. D.; Crooks, R. M. *Anal. Chem.* **2013**, *85*, 9713−9720.
(25) Ge, L.; Wang, S. M.; Song, X. R.; Ge, S. G.; Yu, J. H. *Lab Chip* **2012**, *12*, 3150−3158.
(26) Cybulski, J. S.; Clements, J.; Prakash, M. *PLoS One* **2014**, *9*, e98781.
(27) Lathrop, D. K.; Ervin, E. N.; Barrall, G. A.; Keehan, M. G.; Kawano, R.; Krupka, M. A.; White, H. S.; Hibbs, A. H. *J. Am. Chem. Soc.* **2010**, *132*, 1878−1885.
(28) Bell, P. J.; Karuso, P. *J. Am. Chem. Soc.* **2003**, *125*, 9304−9305.
(29) Hlushkou, D.; Perdue, R. K.; Dhopeshwarkar, R.; Crooks, R. M.; Tallarek, U. *Lab Chip* **2009**, *9*, 1903−1913.
(30) Renkin, E. M. *J. Gen. Physiol.* **1954**, *38*, 225−243.
(31) Kunkel, H. G.; Tiselius, A. *J. Gen. Physiol.* **1951**, *35*, 89−118.
(32) Moghadam, B. Y.; Connelly, K. T.; Posner, J. D. *Anal. Chem.* **2014**, *86*, 5829−5837.
(33) Oh, Y.-J.; Gamble, T. C.; Leonhardt, D.; Chung, C.-H.; Brueck, S. R. J.; Ivory, C. F.; Lopez, G. P.; Petsev, D. N.; Han, S. M. *Lab Chip* **2008**, *8*, 251−258.
(34) Laws, D. R.; Hlushkou, D.; Perdue, R. K.; Tallarek, U.; Crooks, R. M. *Anal. Chem.* **2009**, *81*, 8923−8929.
(35) Wu, J.; Gerstandt, K.; Zhang, H.; Liu, J.; Hinds, B. J. *Nat. Nanotechnol.* **2012**, *7*, 133−139.
(36) Milanova, D.; Chambers, R. D.; Bahga, S. S.; Santiago, J. G. *Electrophoresis* **2011**, *32*, 3286−3294.
(37) Jeppson, J.; Laurell, C.; Franzen, B. *Clin. Chem.* **1979**, *25*, 629−638.
(38) Kyle, R.; Katzmann, J.; Lust, J.; Dispenzieri, A. Clinical Indications and Applications of Electrophoresis and Immunofixation. In *Manual of Clinical Immunology*; Rose, N., Hamiliton, R., Detrick, B., Eds.; ASM Press: Washington DC, 2002; pp 66−70.
(39) Josephson, R.; Mikolajick, E.; Sinha, D. *J. Dairy Sci.* **1972**, *55*, 1508−1510.

(40) Abramson, H. A.; Moyer, L. S.; Gorin, M. H. *Electrophoresis of Proteins and the Chemistry of Cell Surfaces*; Reinhold Publishing: New York, 1942.
(41) Dawson, R. M. C. *Data for Biochemical Research*, 3rd; Clarendon Press: Oxford, 1986.
(42) *The Plasma Proteins: Structure, Function, and Genetic Control*; Putnam, F. W., Ed.; Elsevier: London, 2012; Vol. 3.